

Kinetic Parameters Investigation for The Esterification of Free Fatty Acid from Coconut Oil Mill Waste using Montmorillonite-Sulfonated Carbon from Glucose Composite Catalyst

Hasanudin Hasanudin^{1*}, Wan Ryan Asri¹, Widia Purwaningrum¹, Fahma Riyanti¹, Novia Novia², Roni Maryana³, Muhammad Al Muttaqi³

¹ Biofuel Research Group, Laboratory of Physical Chemistry, Department of Chemistry, Faculty of Mathematics and Natural Science, Universitas Sriwijaya, Indralaya 30662, Indonesia

² Department of Chemical Engineering, Faculty of Engineering, Universitas Sriwijaya, Indralaya 30662, Indonesia

³ Research Center for Chemistry, National Research and Innovation Agency (BRIN-Indonesia), Science and Technology Research Center (PUSPIPTK) Area, Serpong, South Tangerang 15314, Indonesia

*Corresponding author email: hasanudin@mipa.unsri.ac.id

Received June 09, 2022; Accepted September 23, 2022; Available online November 20, 2022

ABSTRACT. Coconut oil mill waste (CMW) contained high free fatty acid (FFA) content which potentially could be converted into a value-added product such as fatty acid methyl ester (FAME). In this study, a montmorillonite-sulfonated carbon catalyst was used to evaluate the kinetic parameter of FFA conversion from CMW into FAME. The characterization of FTIR and SEM-EDX confirmed that the $-SO_3H$ groups were successfully incorporated into the montmorillonite-carbon catalyst. The highest catalyst acidity (9.4 mmol/g) was achieved by a ratio of montmorillonite to sulfonated carbon of 1:3 % w/w. The kinetic study using montmorillonite-sulfonated carbon 1:3 % w/w showed that the reaction temperature and the molar ratio of methanol to FFA (% v/v) were positively correlated to the reaction rate. The highest rate constant of esterification towards the product (k_1), reactant (k_2), and equilibrium were 0.1187, 0.0595, and 1.995, achieved by a temperature of 80 °C, respectively. The Arrhenius constant and activation energy towards the product were 3.3085×10^6 and 50.3 J/mole, respectively. The reaction temperature was positively correlated to the equilibrium constant, which indicated that the reaction was endothermic. The kinetic model validation revealed that the predicted value from the model was adequately in accordance with the experimental value, as indicated by a high coefficient of determination.

Keywords: coconut oil mill waste, free fatty acid, montmorillonite, kinetic study, sulfonated carbon

INTRODUCTION

The quantity of population growth in the world from year to year has increased. Along with the increase in population, the need for fossil fuels will likewise increment (Singh et al., 2022). Individuals utilize petroleum for transportation and industry; hence, it is conceivable that fossil fuel reserves will run out shortly (Akhbari et al., 2021). One solution to overcome this issue is to look for alternative energy sources. Fatty methyl acid ester (FAME) is one of the biofuels that potentially substitute the petroleum reserves because of its biodegradability, non-toxic, and low emission of hazardous exhaust gases (Mohiddin et al., 2021).

Generally, FAME can be produced from a first-generation feedstock such as plant-based, animal, and vegetable oil via transesterification or esterification reactions (Osorio-González et al., 2020). Nonetheless, The competition for the first-generation feedstock between biofuel producers and the food industry is one of the causes of high costs due to expanded food prices and decreased land

accessibility for food crops (Ambat et al., 2018). The second-generation biodiesel feedstock is narrated as a better feedstock due to its non-edible characteristic, which is inherent to cutting back on food shortages (Anwar et al., 2018). Moreover, non-edible oil may be found to be less expensive and abundantly in many world regions, thus offering a sustainable supply (Adenuga et al., 2021). Some commons and non-consumed second-generation FAME feedstocks are castor oil, jatropha oil, cottonseed oil (Atabani et al., 2013), or low-grade oil such as waste cooking oil, sludge, and so forth (Cruz et al., 2018). Among those feedstocks, coconut oil mill waste (CMW) is one alternative feedstock for FAME production. CMW is a low-quality non-edible oil and contains high free fatty acids (FFA), which conceivably can be converted into FAME (Yotsomnuk & Skolpap, 2018). Furthermore, due to its abundance and non-competitive against food, CMW appears, by all accounts, to be a desirable industrial feedstock and can increase the sustainability of the coconut oil industry and diminish its negative environmental impact.

FAME production can be generated by esterification with an acid catalyst (Hayyan et al., 2013). The catalyst frequently utilized is a homogenous acid catalyst. Despite the fact that the homogeneous acid catalyst improves the kinetics, unfortunately, it is undertaking corrosion of the process apparatus, is difficult to separate, and cannot be regenerated, hence increasing production costs (Shaguffa et al., 2017). In the midst of catalyst developments, heterogeneous acid catalysts are very effective and available because they can cover the disadvantages of homogeneous catalysts (Alcañiz-Monge et al., 2018). Many thorough investigations have been conducted in order to generate heterogeneous catalysts from diverse sources and methodologies. One of the heterogeneous catalysts currently developed with excellent and promising performance and high conversion in the esterification of FFA is a sulfonated carbon catalyst (Fauziyah et al., 2020). Sulfonated carbon can be produced by the incomplete carbonization of manageable and simple natural materials such as sugar and biomass, which are directly sulfonated by strong acid (Dornath et al., 2016). Various sulfonated carbon from different precursors have been developed (Farabi et al., 2019; Flores et al., 2019; Lathiya et al., 2018). Among other polymeric materials, glucose as a carbon precursor seems cost-effective due to its abundant readily in nature, porous and appropriate for solid acid catalysts. Moreover, the catalyst will have a much higher catalytic activity when combined with an active supporting material (Hasanudin et al., 2022a). Natural clay such as montmorillonite is widely available, with a high surface area, and has an active catalytic site which has potential as a supporting material that can promote a synergistic effect in the FFA conversion (Varadwaj & Parida, 2013).

Kinetic studies are essential for understanding esterification and promoting industrial application processes. An important structural attribute of a catalyst is related to the rate of the esterification reaction. Several esterification kinetic studies have been reported using various feedstocks and catalysts (Gao et al., 2020; Hamerski et al., 2020; Kusumaningtyas et al., 2017; Liu, Liu, et al., 2019). The previous study employed the zeolite-sulfonated biochar derived from biomass-based such as molasse for the catalytic esterification of FFA derived from sludge palm oil. The study revealed that the reaction had an activation energy of ca. 30.65 kJ/mol towards FAME production, whereas it had an activation energy of ca. 15.87 kJ/mol towards the reversible reaction. This typical reaction took place endothermically with a sufficient kinetics model ($R^2 = 96\%$) (Hasanudin et al., 2022b). The other study also reported that the zeolite-sulfonated carbon derived from sugar cane promoted a ca. 94.19% towards FFA conversion derived from sludge palm oil, optimized by the RSM-CCD method. This catalyst exhibited an adequate reusability

performance for up to 4 consecutive runs (Hasanudin et al., 2022c). According to the literature review, there were neither exploration nor study has been attempted regarding the kinetic study of FFA conversion from CMW into FAME using montmorillonite-sulfonated carbon composite catalyst, with glucose as a carbon source. Apart from what was mentioned earlier, glucose is used as a carbon source because it is easily soluble in water so in the formation of composites, the precursor would be homogeneously mixed with supporting material. Therefore, the aim of this research is to study the kinetics parameter of FFA conversion from CMW to FAME using montmorillonite-sulfonated carbon composite from glucose. The effect of the weight ratio of montmorillonite to glucose (% w/w) was also investigated. The catalyst would be characterized using FT-IR and SEM-EDX. The acidity of the catalyst was calculated using the titration method.

EXPERIMENTAL SECTION

Preparation of Montmorillonite-carbon Composite

Montmorillonite (200-mesh) from PT. Tunas Inti Makmur Semarang was cleaned with distilled water and dried at 120 °C for 1 day. A series of mixtures with various weight ratios of montmorillonite to D(+)-glucose (ca. 97.5-100 % purity, Merck), namely 1:3, 1:2, 1:1, 2:1, and 3:1 (% w/w), was dissolved in distilled water (500 mL) and stirred at 80 °C until homogeneous. Subsequently, the mixture was heated at 120 °C for 24 hours using the oven and carbonized at 500 °C in an N₂ atmosphere with a 2 mL/sec flow rate. The powder was referred to as a montmorillonite-carbon composite.

Sulfonation of Montmorillonite-carbon Composite

Montmorillonite-carbon composite (20 g) was diluted with concentrated H₂SO₄ (100 mL), refluxed at 175 °C for 15 hours, and later washed with distilled water at 80 °C. The mixture was then centrifuged at 500 rpm and dried at 120 °C for 24 hours. This outcome was then called montmorillonite-sulfonated carbon.

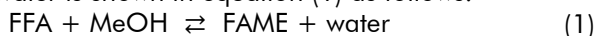
Catalyst Characterization

The acidity of the catalyst was evaluated using the titration method (Nadia et al., 2022). The functional groups of catalyst were assessed using FT-IR (8201 Shimadzu) and the spectra were recorded from 400 cm⁻¹ to 4000 cm⁻¹. The surface morphology of the catalyst was captured using SEM-EDX (JEOL JSM-6510LA).

Kinetic model of esterification

The FFA esterification was modeled according to the first-order pseudo-homogeneous kinetics model. The kinetic study was conducted using a montmorillonite-sulfonated carbon catalyst with the highest acidity. Several assumptions were followed before calculating the kinetics model of the FFA esterification reaction, namely (1) the reactor was

batch system and isothermal (2) the reaction was reversible, and controlled by chemical reactions (3) the rate of non-catalytic reactions was neglected (4) the reaction occurred in the oil phase, and lastly (5) the mole ratio of methanol to oil is sufficiently high, thus the methanol concentration was considered constant throughout the process (Farag et al., 2013). The reaction order for methanol and FFA were considered zero and first order, respectively. The equilibrium reaction of FFA with methanol to produce FAME and water is shown in equation (1) as follows:



Based on the reaction in equation (1), the rate equation can be formulated according to equation (2) as follows:

$$\frac{-d[\text{FFA}]}{dt} = k_1[\text{FFA}][\text{MeOH}] - k_2[\text{FAME}][\text{water}] \quad (2)$$

Where [FFA] and [MeOH] were the free fatty acids concentrations and methanol, respectively, whereas [FAME] and [water] were the concentrations of ester and water, respectively, k_1 and k_2 were the rate constants for the reaction towards the products and the reactants, respectively. Since the methanol concentration was considered constant throughout the process, the equation becomes as follows:

$$\frac{-d[\text{FFA}]}{dt} = k_1[\text{FFA}] - k_2[\text{FAME}]^2 \quad (3)$$

If at the beginning of the reaction ($t=0$) was assumed that the concentration of FAME and water was equal to zero and the concentration of $[\text{FFA}] = [\text{FFA}]_0 - X$, where X was the decrease in acid value. Then equation (3) becomes as follows:

$$\frac{dX}{dt} = k_1([\text{FFA}]_0 - X) - k_2X^2 \quad (4)$$

$[\text{FFA}]_0$ was the initial FFA concentration, and the integration of equation (4) would form the following kinetic equation as follows (Satriana & Supardan, 2008):

$$\ln \left[\left([\text{FFA}]_0 - X \left(\frac{1}{2} + \beta \right) \right) - \left([\text{FFA}]_0 - X \left(\frac{1}{2} - \beta \right) \right) \right] = 2k_2\alpha t \quad (5)$$

Where:

$$\alpha = \left(\frac{K^2}{4} + K [\text{FFA}]_0 \right)^{1/2} \quad (6)$$

$$\beta = \frac{\alpha}{K} \quad (7)$$

The rate constants k_1 and k_2 can be calculated according to the equation (9-10) as follow:

$$k_1 = \frac{\text{Slope}}{2\beta} \quad (8)$$

$$k_2 = \frac{\text{Slope}^2 - k_1^2}{4k_1 [\text{FFA}]_0} \quad (9)$$

Whereas the energy activation and Arrhenius constant of k_1 and k_2 was calculated according to the Arrhenius equation.

Effect of Temperature and Molar Ratio of Methanol to FFA

Esterification was conducted using 25 mL of CMW (PT. Sambu Kuala Enok Riau) and 5 g of a catalyst with mole ratios of methanol to FFA (% v/v), namely, 10:1, 13:1, 16:1, 19:1, and 20:1 in a batch reactor with a temperature of 60, 70, and 80 °C for 60 minutes. The product was taken as much as 2.5 mL at reaction times of 8, 12, 16, 20, and 24 hours. FFA analysis was conducted using the titration method.

Kinetic Model Validation

Validation was carried out to investigate the correspondence between the observed and predicted by a mathematical model of FFA content based on the coefficient of determination. The mathematical model was calculated according to the equation as follows (Farag et al., 2013):

$$Y_{\text{predicted model}} = \frac{[\text{FFA}]_0 (e^{2k_2\alpha t} - 1)}{\beta(1 + e^{2k_2\alpha t}) + 0.5 [\text{FFA}]_0 (e^{2k_2\alpha t} - 1)} \quad (10)$$

RESULTS AND DISCUSSION

Effect of Weight Ratio of Montmorillonite to Glucose

The effect of the ratio of montmorillonite to glucose on montmorillonite-carbon yield is shown in **Figure 1a**. The carbonization of glucose without montmorillonite was led as a control. It can be seen that the montmorillonite-carbon yield reveals a tendency to increment alongside the increase of montmorillonite composition. The highest yield (69.92%) was accomplished at a composition ratio of 3:1. The higher glucose composition produced a relatively low yield of carbon because the glucose was partially carbonized, which promoted the evaporation of a volatile substance and gave a carbon-enriched, porous structure, which was suitable for functionalized by sulfonated groups. Meanwhile, the treatment of glucose carbonization without montmorillonite resulted in a relatively low yield compared to other composition ratios, which were associated with high volatilization of glucose structure, leading to a low carbon yield. This condition confirmed that the addition of montmorillonite to glucose affected the carbon yield, which inherently affected the carbon structure.

The montmorillonite-carbon catalyst is subsequently sulfonated, and its acidity values are shown in **Figure 1b**. It was revealed that a higher glucose ratio caused an increase in catalyst acidity. The montmorillonite-sulfonated carbon composite catalyst with a ratio of 1:3 had the highest acidity (9.4 mmol/g) compared to other compositions. Higher glucose content as a carbon source exhibited more -SO₃H groups bounded to the catalyst, leading to increased catalysts acidity that provides the high catalytic activity.

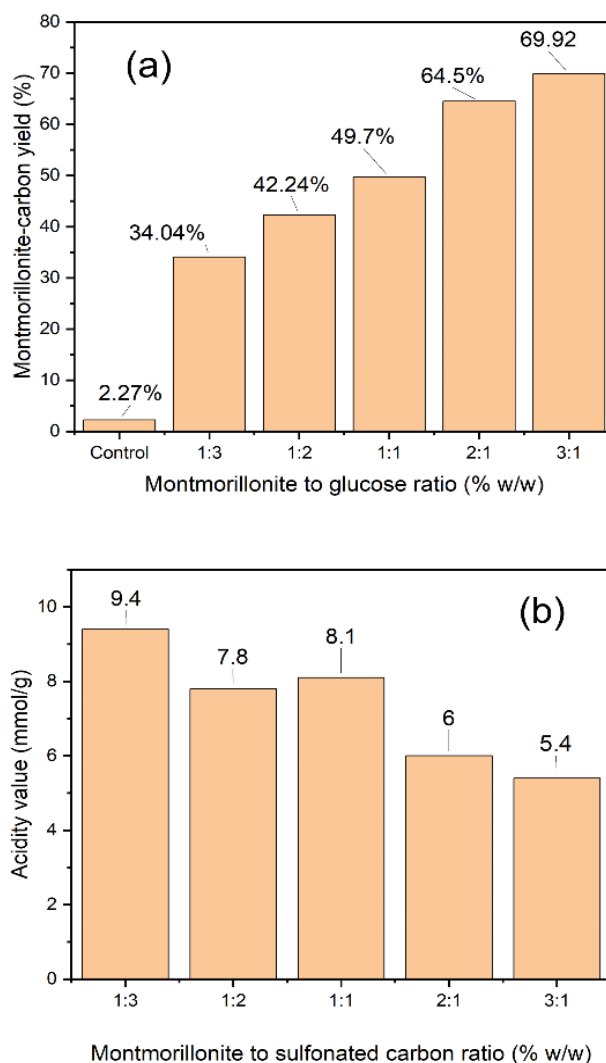


Figure 1. (a) The effect of the montmorillonite to glucose ratio on montmorillonite-carbon yield (b) Montmorillonite-sulfonated carbon composite catalyst acidity.

Characterization of Catalysts

FT-IR was used to investigate the functional groups of catalysts. The spectra of montmorillonite-sulfonated carbon catalysts are shown in **Figure 2**. The spectra of montmorillonite-sulfonated carbon 1:3 from **Figure 2a** revealed an absorption band at 1065.71 cm^{-1} , which indicated the SO_3H group bounded to the carbon surface (Li et al., 2018). The absorption band at 3448.72 cm^{-1} corresponded to the vibration of the OH group, which was probably from the $(-\text{S}=\text{O})(\text{OH})$ group. Furthermore, a stretching vibration of C-S-C was observed at 794.67 cm^{-1} (Ogino et al., 2018). These conditions indicated that the catalyst had been successfully sulfonated. The absorption band at 1635 cm^{-1} was attributed to the carbonyl vibration of the COOH group and might overlap with the C=C absorption in the polyaromatic structure (Chen & Fang, 2011). The absorption band at 462.92 cm^{-1} , 794.67 cm^{-1} , and 339 cm^{-1} indicated the vibration of Si-O-Al (Liu, Zeng, et al., 2019), which was probably from alumina-silica montmorillonite typical structure, as well as the overlap of bending vibration of aromatic

C-H (Alshabanat et al., 2013). This condition indicated that there was an interaction between carbon and montmorillonite structure. This interaction suggested that the montmorillonite was coated by carbon, whereas the sulfonated groups were functionalized in the carbon framework. **Figure 2b** and **Figure 2c** showed relatively similar absorption bands and were not significantly different from **Figure 2a**. Furthermore, the intensity of the absorption band in the $\sim 1060\text{ cm}^{-1}$ region (SO_3H groups) increased along with the increase of glucose composition, and this condition indicated that the montmorillonite-sulfonated carbon (1:3) composite catalyst through FTIR analysis, had the highest acidity and these findings were consistent with acidity analysis as well.

The images of catalyst morphology surface using SEM and EDX analysis are shown in **Figure 3**. It was apparent from **Figure 3a** that the surface morphology seems to be an undulating thin layer, which was typical of montmorillonite (Goodarzi et al., 2016). The surface morphology of sulfonated carbon in **Figure 3b** exhibited an irregular shape. The sulfonation process

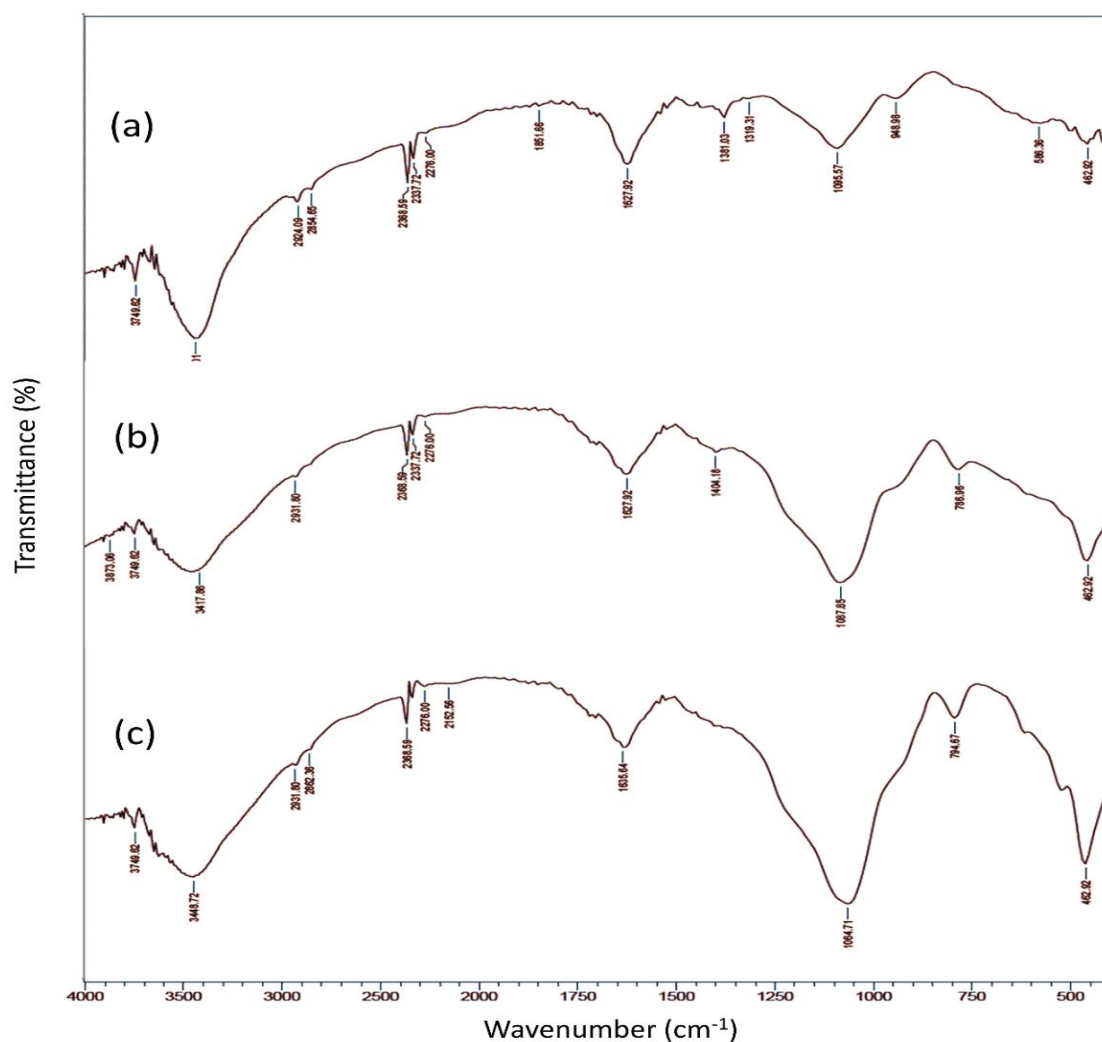


Figure 2. FT-IR spectra of montmorillonite-sulfonated carbon (a) 1:3 (b) 1:1, and (c) 3:1 (% w/w).

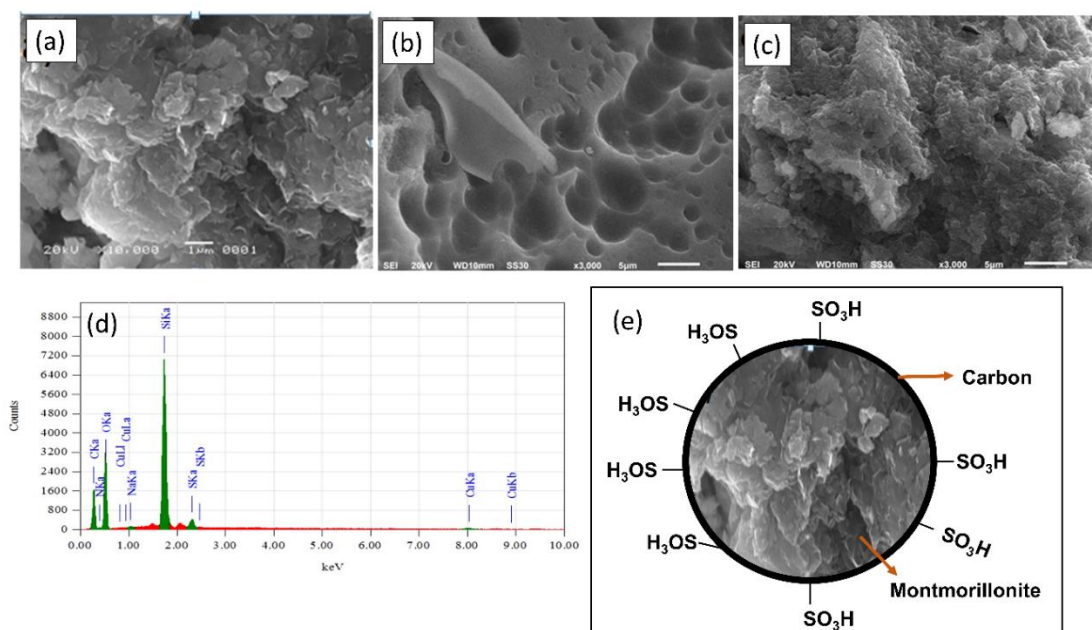


Figure 3. SEM images of (a) Natural montmorillonite (b) Sulfonated carbon (c) Montmorillonite-sulfonated carbon (1:3) (d) EDX spectra of Montmorillonite-sulfonated carbon (1:3) (e) The proposed scheme of montmorillonite-sulfonated carbon composite.

caused changes in the carbon pores (Hajamini et al., 2016). The montmorillonite-sulfonated carbon (1:3) in **Figure 3c** formed a rough round lump, and the morphological surface had a similar image to natural montmorillonite (**Figure 3a**), which indicated the composite formation was successful. Furthermore, EDX analysis of montmorillonite-sulfonated carbon showed sulfur content of 1.16%, presumably from SO_3H groups, which indicated the montmorillonite-carbon catalyst had been successfully sulfonated. **Figure 3e** shows the proposed scheme of montmorillonite-sulfonated carbon composite. It was suggested that the montmorillonite was coated by carbon, whereas the sulfonated groups were functionalized in the carbon framework.

Kinetic Studies

The effect of temperature and the molar ratio methanol to FFA on the esterification reaction rate is revealed in **Figure 4**. It can be seen that **Figure 4** shows that the rate of the esterification gradually incremented as the reaction temperature increased. From this study, the highest reaction rate was accomplished at a temperature of 80 °C, whereas the lowest reaction rate was achieved at a temperature of 60 °C. An increase in temperature provided energy to the molecules; thus, the reaction rate would be faster, and this condition caused the frequency of collisions between molecules to be higher (Gao et al., 2020). The collision model explained why the reaction rate was faster at higher temperatures. Subsequently, **Figure 4** shows that the rate of the esterification reaction was inversely proportional to the mole ratio of methanol to FFA, which implied that the reaction rate decreased as the mole ratio is increased. With the higher mole ratio of methanol to FFA, the initial FFA content would be lower, whereas the reaction volume was increased with a constant catalyst dosage; This condition caused the possibility of a collision between the FFA and the catalyst acquire to be smaller, making the reactants activated by the catalyst was more

difficult to form, thus the reaction rate was slower. According to Cao et al. (2021), excessive methanol can also over-dilute the reaction system's concentration, limiting the possibility of FFA reaching the active catalytic site.

The effect of temperature on reaction rate and equilibrium constant are shown in **Figure 5** respectively. It can be seen that at a relatively low reaction temperature (60 °C), the esterification reaction generated a lower reaction rate constant towards the product (k_1) than the reverse reaction towards the reactant (k_2), which indicated that the esterification FFA into the product (FAME) was slower than the reverse reaction. Consequently, the formation of high content of FAME in this condition was likely unfavorable. Subsequently, **Figure 7b** reveals that when the reaction temperature was incremented to 70 °C, the reaction rate constants of k_1 and k_2 did not differ significantly. This condition indicated that the esterification towards the products was almost as fast as the reverse reaction. Furthermore, the temperature increased by 80 °C (**Figure 5**), was promoted a higher forward rate constant towards the product (k_1) than the reverse reaction (k_2). In this condition, the esterification runs most optimally; this was associated with faster molecular motion and higher kinetic energy; thus, more collisions between reactant molecules occurred and increased the reaction rate (Mekala & Goli, 2015).

The average value of the reaction rate of k_1 , k_2 and the equilibrium constant for each temperature are presented in **Table 1**, respectively. According to Le Chatelier's principle, if the equilibrium reaction's temperature is increased, the reaction equilibrium will shift towards the endothermic reaction (Jagadeeshbabu et al., 2011). As indicated by this study, the higher the temperature, the greater the value of the equilibrium constant (K). This condition showed that the esterification reaction of FFA from CMW with methanol was an endothermic reaction and consistent with another report (Su, 2013) previously.

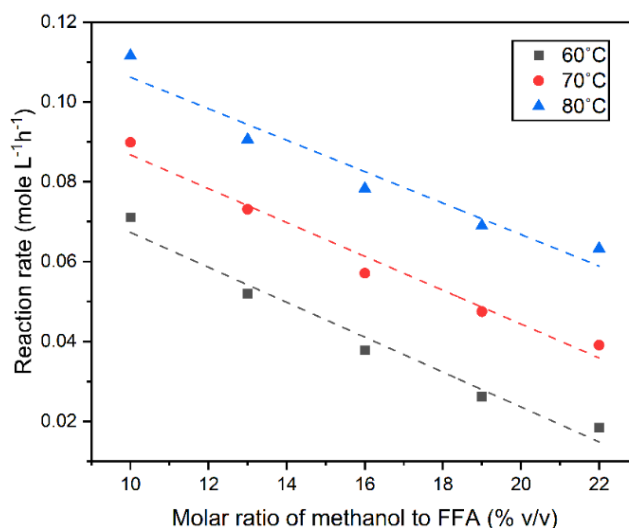


Figure 4. The effect of temperature and the molar ratio of methanol to FFA on reaction rate.

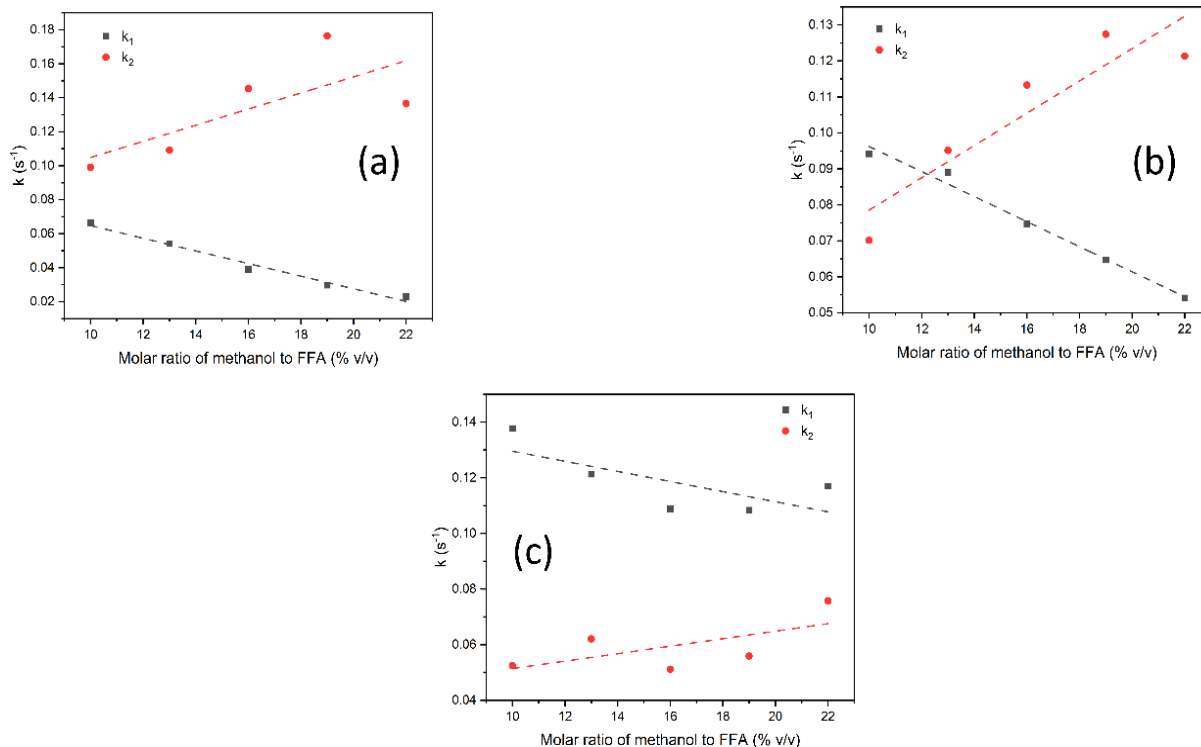


Figure 5. The effect of temperature and molar ratio of methanol to FFA on reaction rate constant at (a) 60 °C (b) 70 °C (c) 80 °C.

Table 1. Average value of reaction rate constant for each temperature

Reaction temperature (°C)	Average value		K
	k_1	k_2	
60	0.0425	0.1333	0.3184
70	0.0754	0.1055	0.7144
80	0.1187	0.0595	1.9955

Arrhenius Constant and Energy Activation Analysis

The esterification reaction occurred when there were intermolecular collisions at the active site of the molecule and the active site of the catalyst. After reactants collided, they would form products. A large complex of reactant molecules would cause minor collisions on the active site and vice versa (Setyaningsih et al., 2019). This factor is determined by the collision frequency factor, expressed by the Arrhenius constant. The Arrhenius constant (A) was evaluated from the intercept derived from the plot of $1/T$ respect to $\ln k_1$, whereas the activation energy (E_a) was evaluated from the slope (Figure 6).

The results of the analysis of the Arrhenius constant in Figure 6, it was found that the collision frequency of the esterification of FFA from CMW and methanol with a montmorillonite-sulfonated carbon catalyst was 3.3085×10^6 . The activation energy of FFA esterification from CMW towards product was found to be 50.3 J/mol. The activation energy acquired was relatively small, which indicated that the catalyst had high catalytic activity towards FFA esterification, thus the reaction easily occurred (Lu et al., 2014). The

molecular fraction which had energy equal to or greater than E_a is shown in Table 2. It was conspicuous that by increasing the reaction temperature, the molecular fraction also increases. This condition shows that the greater reactant molecular fraction, leading to an increase in the probability of the formation of a FAME.

Kinetic Model Validation

The validation of the kinetic model was conducted to prove the results of the predicted calculation by the model of the FFA reduction were matched the experimental calculation (Gao et al., 2020). Figure 7 shows the linear regression of FFA esterification between the predicted value calculated by kinetic model and experimental value with a coefficient of determination obtained of 0.9803. This regression value was close to 1, indicated that the predicted value from a kinetic model of FFA reduction was in accordance with the experimental value (Su, 2013). This condition justified that the proposed FFA kinetics model from CMW using montmorillonite-sulfonated carbon could be used to predict the FFA reduction from CMW with high precision.

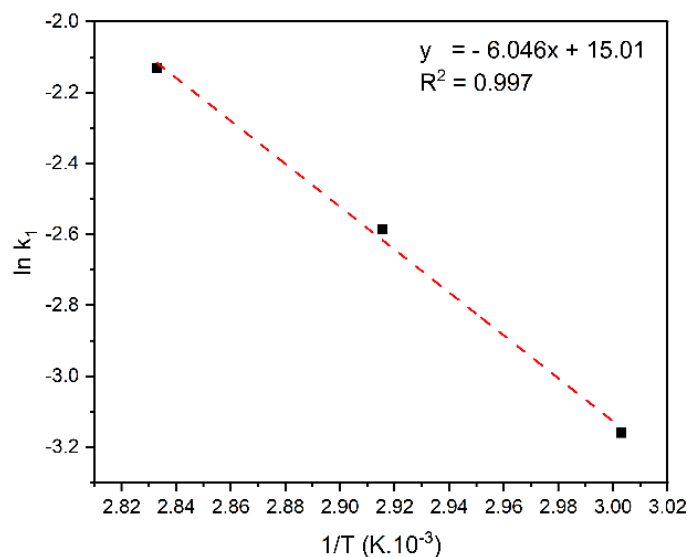


Figure 6. Plot of 1/T respect to $\ln k_1$.

Table 2. Molecular fraction with equal to or greater than activation energy

Reaction temperature (°C)	$f(e^{-E_a/RT})$
60	0.9819
70	0.9825
80	0.9830

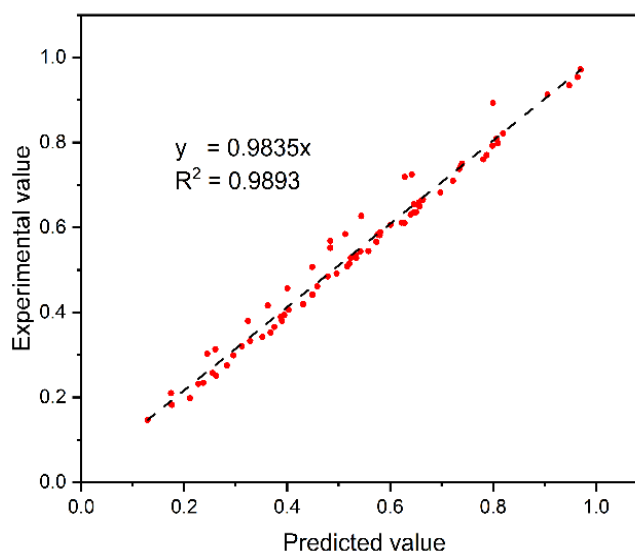


Figure 7. Linear regression of predicted value vs experimental value.

CONCLUSIONS

The montmorillonite-sulfonated carbon has been developed for catalyzing the FFA conversion from CMW into FAME. FTIR and SEM-EDX analysis confirmed the presence of $-SO_3H$ groups on montmorillonite-sulfonated carbon catalyst. The highest acidity (9.4 mmol/g) was achieved by montmorillonite-sulfonated carbon with a ratio of montmorillonite to sulfonated carbon of 1:3 % w/w. The kinetic study showed that the highest rate reaction of FFA esterification from CMW using montmorillonite-sulfonated carbon 3:1 % w/w was

achieved at a reaction temperature of 80 °C and methanol to FFA molar ratio of 22:1. The highest rate constant of esterification towards the product (k_1), reactant (k_2), and equilibrium were 0.1187, 0.0595, and 1.995, achieved by a temperature of 80 °C, respectively with an endothermic reaction. The constant Arrhenius and activation energy towards product were obtained of 3.3085×10^6 and 50.3 J/mol. The kinetic model validation showed that the predicted value generated by the model was in accordance with the experimental study.

ACKNOWLEDGMENTS

The author wishes to express gratitude to all members of the Biofuel Research Group, Laboratory of Physical Chemistry, Department of Chemistry, Universitas Sriwijaya, who contributed to this research.

REFERENCES

- Adenuga, A. A., Oyekunle, J. A. O., & Idowu, O. O. (2021). Pathway to reduce free fatty acid formation in *Calophyllum inophyllum* kernel oil: A renewable feedstock for biodiesel production. *Journal of Cleaner Production*, 316, 128222.
- Akhbari, A., Onn, C. C., & Ibrahim, S. (2021). Analysis of biohydrogen production from palm oil mill effluent using a pilot-scale up-flow anaerobic sludge blanket fixed-film reactor in life cycle perspective. *International Journal of Hydrogen Energy*, 46(68), 34059–34072.
- Alcañiz-Monge, J., Bakkali, B. El, Trautwein, G., & Reinoso, S. (2018). Zirconia-supported tungstophosphoric heteropolyacid as heterogeneous acid catalyst for biodiesel production. *Applied Catalysis B: Environmental*, 224, 194–203.
- Alshabanat, M., Al-Arrash, A., & Mekhamer, W. (2013). Polystyrene/montmorillonite nanocomposites: Study of the morphology and effects of sonication time on thermal stability. *Journal of Nanomaterials*, 2013, 650725.
- Ambat, I., Srivastava, V., & Sillanpää, M. (2018). Recent advancement in biodiesel production methodologies using various feedstock: A review. *Renewable and Sustainable Energy Reviews*, 90, 356–369.
- Anwar, M., Rasul, M. G., Ashwath, N., & Rahman, M. M. (2018). Optimisation of second-generation biodiesel production from Australian native stone fruit oil using response surface method. *Energies*, 11(10), 2655.
- Atabani, A. E., Mahlia, T. M. I., Badruddin, I. A., Masjuki, H. H., Chong, W. T., & Lee, K. T. (2013). Investigation of physical and chemical properties of potential edible and non-edible feedstocks for biodiesel production, a comparative analysis. *Renewable and Sustainable Energy Reviews*, 21, 749–755.
- Cao, M., Peng, L., Xie, Q., Xing, K., Lu, M., & Ji, J. (2021). Sulfonated *Sargassum horneri* carbon as solid acid catalyst to produce biodiesel via esterification. *Bioresource Technology*, 324, 124614.
- Chen, G., & Fang, B. (2011). Preparation of solid acid catalyst from glucose-starch mixture for biodiesel production. *Bioresource Technology*, 102(3), 2635–2640.
- Cruz, M., Pinho, S. C., Mota, R., Almeida, M. F., & Dias, J. M. (2018). Enzymatic esterification of acid oil from soapstocks obtained in vegetable oil refining: Effect of enzyme concentration. *Renewable Energy*, 124, 165–171.
- Dornath, P., Ruzycky, S., Pang, S., He, L., Dauenhauer, P., & Fan, W. (2016). Adsorption-enhanced hydrolysis of glucan oligomers into glucose over sulfonated three-dimensionally ordered mesoporous carbon catalysts. *Green Chemistry*, 18(24), 6637–6647.
- Farabi, M. S. A., Ibrahim, M. L., Rashid, U., & Taufiq-Yap, Y. H. (2019). Esterification of palm fatty acid distillate using sulfonated carbon-based catalyst derived from palm kernel shell and bamboo. *Energy Conversion and Management*, 181, 562–570.
- Farag, H. A., El-Maghraby, A., & Taha, N. A. (2013). Kinetic study of used vegetable oil for esterification and transesterification process of biodiesel production. *International Journal of Chemical and Biochemicals Sciences*, 3, 1–8.
- Fauziyah, M., Widiyastuti, W., & Setyawan, H. (2020). Sulfonated carbon aerogel derived from coir fiber as high performance solid acid catalyst for esterification. *Advanced Powder Technology*, 31(4), 1412–1419.
- Flores, K. P., Omega, J. L. O., Cabatingan, L. K., Go, A. W., Agapay, R. C., & Ju, Y. H. (2019). Simultaneously carbonized and sulfonated sugarcane bagasse as solid acid catalyst for the esterification of oleic acid with methanol. *Renewable Energy*, 130, 510–523.
- Gao, X., Ding, Q., Wu, Y., Jiao, Y., Zhang, J., Li, X., & Li, H. (2020). Kinetic study of esterification over structured ZSM-5-coated catalysts based on fluid flow situations in macrocellular foam materials. *Reaction Chemistry and Engineering*, 5(3), 485–494.
- Goodarzi, A. R., Najafi Fateh, S., & Shekary, H. (2016). Impact of organic pollutants on the macro and microstructure responses of Na-bentonite. *Applied Clay Science*, 121–122, 17–28.
- Hajamini, Z., Sobati, M. A., Shahhosseini, S., & Ghobadian, B. (2016). Waste fish oil (WFO) esterification catalyzed by sulfonated activated carbon under ultrasound irradiation. *Applied Thermal Engineering*, 94, 1–10.
- Hamerski, F., Dusi, G. G., dos Santos, J. T. F., da Silva, V. R., Voll, F. A. P., & Corazza, M. L. (2020). Esterification reaction kinetics of acetic acid and n-pentanol catalyzed by sulfated zirconia. *International Journal of Chemical Kinetics*, 52(8), 499–512.
- Hasanudin, H., Asri, W. R., Bahrain, D., & Fitri, H. (2022c). Esterification of free fatty acid from sludge palm oil using zeolite-sulfonated carbon from sugar cane catalysts. *Journal of Oil Palm Research*. (In Press).
- Hasanudin, H., Asri, W. R., Meilani, A., & Yuliasari, N. (2022b). Kinetics study of free fatty acid

- esterification from sludge palm oil using zeolite sulfonated biochar from molasses composite catalyst. *Material Science Forum*, 1061, 113–118.
- Hasanudin, H., Putri, Q. U., Agustina, T. E., & Hadiah, F. (2022a). Esterification of free fatty acid in palm oil mill effluent using sulfated carbon-zeolite composite catalyst. *Pertanika Journal of Science & Technology*, 30(1), 377–395.
- Hayyan, A., Hashim, M. A., Mirghani, M. E. S., Hayyan, M., & AlNashef, I. M. (2013). Esterification of sludge palm oil using trifluoromethanesulfonic acid for preparation of biodiesel fuel. *Korean Journal of Chemical Engineering*, 30(6), 1229–1234.
- Jagadeeshbabu, P. E., Sandesh, K., & Saidutta, M. B. (2011). Kinetics of esterification of acetic acid with methanol in the presence of ion exchange resin catalysts. *Industrial and Engineering Chemistry Research*, 50(12), 7155–7160.
- Kusumaningtyas, R. D., Ratrianti, N., Purnamasari, I., & Budiman, A. (2017). Kinetics study of Jatropha oil esterification with ethanol in the presence of tin (II) chloride catalyst for biodiesel production. In *AIP Conference Proceedings* (Vol. 1788, No. 1, p. 030086). AIP Publishing LLC.
- Lathiya, D. R., Bhatt, D. V., & Maheria, K. C. (2018). Synthesis of sulfonated carbon catalyst from waste orange peel for cost effective biodiesel production. *Bioresource Technology Reports*, 2, 69–76.
- Li, X., Shu, F., He, C., Liu, S., Leksawasdi, N., Wang, Q., Qi, W., Alam, M. A., Yuan, Z., & Gao, Y. (2018). Preparation and investigation of highly selective solid acid catalysts with sodium lignosulfonate for hydrolysis of hemicellulose in corncob. *RSC Advances*, 8(20), 10922–10929.
- Liu, Ying, Liu, J., Yan, H., Zhou, Z., & Zhou, A. (2019). Kinetic Study on esterification of acetic acid with isopropyl alcohol catalyzed by ion exchange resin. *ACS Omega*, 4(21), 19462–19468.
- Liu, Yunxia, Zeng, F., Sun, B., Jia, P., & Graham, I. T. (2019). Structural characterizations of aluminosilicates in two types of fly ash samples from Shanxi Province, North China. *Minerals*, 9(6), 358.
- Lu, X., Yin, H., Shen, L., Feng, Y., Wang, A., Shen, Y., Hang, H., & Mao, D. (2014). Reaction kinetics of the esterification reaction between ethanol and acetic acid catalyzed by Keggin heteropolyacids. *Reaction Kinetics, Mechanisms and Catalysis*, 111(1), 15–27.
- Mekala, M., & Goli, V. R. (2015). Kinetics of esterification of methanol and acetic acid with mineral homogeneous acid catalyst. *Chinese Journal of Chemical Engineering*, 23(1), 100–105.
- Mohiddin, M. N. Bin, Tan, Y. H., Seow, Y. X., Kansedo, J., Mubarak, N. M., Abdullah, M. O., Chan, Y. S., & Khalid, M. (2021). Evaluation on feedstock, technologies, catalyst and reactor for sustainable biodiesel production: A review. *Journal of Industrial and Engineering Chemistry*, 98, 60–81.
- Nadia, A., Wijaya, K., Falah, I. I., Sudiono, S., & Budiman, A. (2022). Self-regeneration of Monodisperse Hierarchical Porous NiMo/Silica Catalyst Induced by NaHCO₃ for Biofuel Production. *Waste and Biomass Valorization*, 13, 2335–2347.
- Ogino, I., Suzuki, Y., & Mukai, S. R. (2018). Esterification of levulinic acid with ethanol catalyzed by sulfonated carbon catalysts: Promotional effects of additional functional groups. *Catalysis Today*, 314, 62–69.
- Osorio-González, C. S., Gómez-Falcon, N., Sandoval-Salas, F., Saini, R., Brar, S. K., & Ramírez, A. A. (2020). Production of biodiesel from castor oil: A review. *Energies*, 13(10), 1–22.
- Satriana, S., & Supardan, M. D. (2008). Kinetic study of esterification of free fatty acid in low grade crude palm oil using sulfuric acid. *ASEAN Journal of Chemical Engineering*, 8(1 & 2), 1–8.
- Setyaningsih, L., Mutiara, T., Chafidz, A., Zulkania, A., Andrianto, M. A., & Farikha, N. L. (2019). Kinetic modelling of esterification of glycerol with acetic acid catalyzed by lewatiite. In *IOP Conference Series: Materials Science and Engineering* (Vol. 543, No. 1, p. 012008). IOP Publishing.
- Shagufta, Ahmad, I., & Dhar, R. (2017). Sulfonic acid-functionalized solid acid catalyst in esterification and transesterification reactions. *Catalysis Surveys from Asia*, 21(2), 53–69.
- Singh, S., Pandey, D., Saravanabhupathy, S., Daverey, A., Dutta, K., & Arunachalam, K. (2022). Liquid wastes as a renewable feedstock for yeast biodiesel production: Opportunities and challenges. *Environmental Research*, 207, 112100.
- Su, C. H. (2013). Kinetic study of free fatty acid esterification reaction catalyzed by recoverable and reusable hydrochloric acid. *Bioresource Technology*, 130, 522–528.
- Varadwaj, G. B. B., & Parida, K. M. (2013). Montmorillonite supported metal nanoparticles: An update on syntheses and applications. *RSC Advances*, 3(33), 13583–13593.
- Yotsomnuk, P., & Skolpap, W. (2018). Effect of process parameters on yield of biofuel production from waste virgin coconut oil. *Engineering Journal*, 22(6), 21–35.